The FreeEOS Code for Calculating the Equation of State for Stellar Interiors II: Efficient Solution Using the Equilibrium-Constant Approach

Alan W. Irwin

Department of Physics and Astronomy, University of Victoria,
P.O. Box 3055, Victoria, British Columbia, Canada, V8W 3P6
Electronic mail: irwin@uvastro.phys.uvic.ca

ABSTRACT

This paper describes an efficient method for minimizing the free energy. The implementation of this method is central to FreeEOS (http://freeeos.sourceforge.net/), a software package for calculating the equation of state for physical conditions in stellar interiors.

Subject headings: free-energy minimization — equation of state — stellar interiors — stellar evolution

1. Introduction

FreeEOS (http://freeeos.sourceforge.net/) is a software package for calculating the equation of state (hereafter, EOS) for stellar conditions. Paper I (Irwin 2004) in this series described the high-quality Fermi-Dirac integral approximations used in the FreeEOS implementation. Here for the second paper in this series, I present an efficient method based on equilibrium constants for minimizing the various user-selected free-energy models available for FreeEOS. The method is a straightforward extension of the equilibrium-constant approach used for calculating the EOS for stellar atmospheres that accounts fully for non-ideal effects for stellar-interior conditions in a thermodynamically consistent way.

For a given Helmholtz free-energy model, chemical equilibrium is traditionally obtained for detailed EOS calculations such as those of Mihalas, Däppen, & Hummer 1988 (hereafter, MDH) by adjusting the number densities of the various species in such a way that the free energy is minimized subject to the usual constraints of abundance conservation and charge neutrality. The present technique satisfies the same equations but reformulates them in terms of equilibrium constants. This greatly reduces the number of variables (the so-called auxiliary variables of the technique) that need to be adjusted to find chemical equilibrium. The result is a FreeEOS implementation which is so efficient that it can be easily be calculated on a low-end PC. (The FreeEOS code was originally developed on a Pentium-133.)

The remainder of this paper is organized as follows: Section 2 presents, in a convenient notation, the constraint equations that must be satisfied by an EOS calculation; Section 3 shows that the

equilibrium-constant approach for minimizing the free energy yields thermodynamically consistent results; Section 4 presents the general formula for equilibrium constants; Section 5 gives a general discussion of the auxiliary variables that must be known in order to calculate non-ideal corrections to the equilibrium constants; Section 6 describes how the EOS is solved with the equilibrium-constant approach; Section 7 gives results and discussion, while Section 8 concludes.

2. The Constraint Equations

An EOS must satisfy abundance conservation and charge neutrality constraints. An example of such constraints (where for illustrative purposes I ignore all species other than free electrons and the more important hydrogen and helium species) is as follows:

$$2N(\mathrm{H}_2^+) + 2N(\mathrm{H}_2) + N(\mathrm{H}) + N(\mathrm{H}^+) = MN_0\ X(\mathrm{H})/A(\mathrm{H}), \tag{1}$$

$$N(\mathrm{He}) + N(\mathrm{He}^+) + N(\mathrm{He}^{++}) = MN_0\ X(\mathrm{He})/A(\mathrm{He}), \tag{2}$$

and

$$N_e - N(\mathrm{H}_2^+) - N(\mathrm{H}^+) - N(\mathrm{He}^+) - 2N(\mathrm{He}^{++}) = 0. \tag{3}$$

The symbols in these constraint equations have the following meanings: N_0 is Avogadro's number; all other N symbols stand for the number of particles of the specified type within the volume V; M is the mass within the volume; while the X and A symbols respectively stand for the abundance by weight and atomic weight of the element of specified type. From the charge neutrality constraint given by equation (3) every positive ion has associated with it sufficient free electrons to neutralize its charge. Thus, the right-hand sides of equations (1) and (2) are the mass of the particular element (including bound electrons and associated free electrons that neutralize the charge of the positive ion forms of the element) within the volume divided by the mass per particle of the neutral monatomic form of the element. These right-hand sides therefore reduce to the number of nuclei (whether bound into molecules or not) of the given species in the volume, and are therefore equal to the corresponding left-hand sides of equations (1) and (2).

I generalize the above notation to a large number of different species made up of many elements as follows: for arbitrary abundance mixtures of k_{elem} elements, the k_{elem} abundance conservation constraint equations and the charge neutrality constraint equation are given by

$$\sum_\sigma N_\sigma C_{\sigma j} = MN_0\ \epsilon_j \tag{4}$$

(see also MDH, eqs. [20], [22], and [23]); where $j = 1, \ldots, k_{\mathrm{elem}} + 1$; N_σ is the number of particles of species type σ in the volume, and σ ranges over all species including electrons. The special index $j = k_{\mathrm{elem}} + 1$ refers to the charge neutrality equation with a formal $\epsilon_{k_{\mathrm{elem}}+1} \equiv 0$. Otherwise, for the element indexed by $j \le k_{\mathrm{elem}}$

$$\epsilon_j \equiv X_j/A_j \equiv \nu_j \sum_k X_k/A_k \equiv \nu_j / \sum_k \nu_k A_k, \tag{5}$$

where X_j ($\equiv \nu_j A_j / \sum_k \nu_k A_k$) is the relative abundance by mass, ν_j ($\equiv [X_j/A_j] / \sum_k [X_k/A_k]$) is the relative abundance by number, and A_j is the atomic weight.

The $C_{\sigma j}$ are stoichiometric coefficients that keep track of how many times species of type σ contributes to the constraint equation of type j. For $j \leq k_{\rm elem}$, $C_{\sigma j}$ is the number of atoms of the jth reference element contained by species σ. For $j = e \equiv k_{\rm elem} + 1$, $C_{\sigma e}$ is the negative charge (or the negative of the positive charge) of the species σ. The stoichiometric coefficients are easy to determine for each species included in the EOS. For example, from equations (1) and (3) the stoichiometric coefficients of H_2^+ are 2 for the hydrogen conservation equation, -1 for the charge neutrality equation and zero for all other constraint equations, and the stoichiometric coefficients of the free electron are 1 for the charge neutrality equation and zero for all other constraint equations.

3. Thermodynamic Consistency

For free energy F, temperature, T, and arbitrary $\vec{N}$, which is not necessarily in chemical equilibrium, the following well-known definitions apply:

$$P(T, V, \vec{N}) \equiv -\partial F(T, V, \vec{N})/\partial V, \tag{6}$$

$$S(T, V, \vec{N}) \equiv -\partial F(T, V, \vec{N})/\partial T, \tag{7}$$

and

$$U(T, V, \vec{N}) \equiv F(T, V, \vec{N}) + TS(T, V, \vec{N}), \tag{8}$$

where P is the pressure, S and U are the entropy and internal energy in V, and $\vec{N}$ is the number vector with components N_σ (see eq. [4]). These equations satisfy Maxwell's relations so all thermodynamic relations are guaranteed to hold true at fixed $\vec{N}$. This is what is meant by thermodynamic consistency. When $\vec{N}$ is not fixed but instead determined from chemical equilibrium constraints implicitly as a function of T, V, M, and $\vec{\epsilon}$ it turns out that thermodynamic consistency still holds (see related discussion in Sect. 9.12 of Cox & Giuli 1968). The purpose of this section is to present a derivation of this fundamental result for the present equilibrium-constant method of minimizing the free energy.

The derivation requires a notation that distinguishes between the parts of $\vec{N}$ which refer to reference and non-reference species. The reference part is designated $\vec{N}^{\mathbf{r}}$ and consists of the $k_{\rm elem}+1$ reference species which are chosen to be the neutral monatomic form of each element and the free electron. The order of the reference species is the same order as the corresponding constraint equations with the free electron corresponding to the charge neutrality equation. The remaining non-reference part of $\vec{N}$ is designated $\vec{N}^{\mathbf{nr}}$. Straightforward manipulation of the constraint equations (eq. [4]) allows expressing the reference numbers as a function of abundance, mass, and the non-reference numbers;

$$\vec{N}^{\mathbf{r}} = \vec{N}^{\mathbf{r}}(\vec{\epsilon}, M, \vec{N}^{\mathbf{nr}}). \tag{9}$$

The partial derivatives (for $j = 1, \ldots, k_{\rm elem} + 1$ and $\sigma = k_{\rm elem} + 2, \ldots, k_{\rm spec}$ with $k_{\rm spec}$ defined to be the number of different species) are given by

$$\partial N_j^{\mathbf{r}}(\vec{\epsilon}, M, \vec{N}^{\mathbf{nr}})/\partial N_\sigma^{\mathbf{nr}} = -C_{\sigma j}. \tag{10}$$

Note these partial derivatives are greatly simplified by the choice of reference species which have stoichiometric coefficients of unity with respect to their associated constraint equations and zero with respect to the remaining constraint equations.

The condition of chemical equilibrium implies that $\vec{N}^{\mathbf{nr}}$ must be varied to minimize

$$F(T, V, \vec{\epsilon}, M, \vec{N}^{\mathbf{nr}}) = F[T, V, \vec{N}^{\mathbf{r}}(\vec{\epsilon}, M, \vec{N}^{\mathbf{nr}}), \vec{N}^{\mathbf{nr}}]. \tag{11}$$

At that minimum

$$\partial F(T, V, \vec{\epsilon}, M, \vec{N}^{\mathbf{nr}})/\partial N_\sigma^{\mathbf{nr}} = 0. \tag{12}$$

Applying the chain rule to this equation and using equation (10) gives (for $\sigma = k_{\rm elem} + 2, \ldots, k_{\rm spec}$)

$$\mu_\sigma = \sum_{j=1}^{k_{\rm elem}+1} C_{\sigma j}\mu_j \tag{13}$$

(see also MDH, eqs. [13]–[16] and [21]), where the chemical potentials are defined in the usual way (for $k = 1, \ldots, k_{\rm spec}$) by

$$\mu_k(T, V, \vec{N}) \equiv \partial F(T, V, \vec{N})/\partial N_k. \tag{14}$$

Equation (13) is a fundamental relationship between chemical potentials of non-reference and reference species at chemical equilibrium where the free energy is minimized. I transform this relationship in Section 4 to derive the relationship between number densities and equilibrium constants that is the basis of the present method of minimizing the free energy. Here I use equation (13) to prove thermodynamic consistency at chemical equilibrium.

At chemical equilibrium $\vec{N}_{\mathbf{eq}}^{\mathbf{nr}}$ is an implicit function of T, V, $\vec{\epsilon}$, and M; and the equilibrium value of the free energy is defined by

$$\begin{aligned} F_{\rm eq}(T, V, \vec{\epsilon}, M) &\equiv F(T, V, \vec{N}_{\rm eq}) \\ &\equiv F\{T, V, \vec{N}^{\mathbf{r}}[\vec{\epsilon}, M, \vec{N}_{\mathbf{eq}}^{\mathbf{nr}}(T, V, \vec{\epsilon}, M)], \vec{N}_{\mathbf{eq}}^{\mathbf{nr}}(T, V, \vec{\epsilon}, M)\}. \end{aligned} \tag{15}$$

Applying the chain rule to the last version of this equation and using equations (10), (13), and (14) gives

$$\begin{aligned}
\partial F_{\rm eq}(T,V,\vec{\epsilon},M)/\partial V &= \partial F(T,V,\vec{N}_{\rm eq})/\partial V \\
&\quad - \sum_{j=1}^{k_{\rm elem}+1} \mu_j \sum_{\sigma=k_{\rm elem}+2}^{k_{\rm spec}} C_{\sigma j}\partial N_{\rm eq}(T,V,\vec{\epsilon},M)_\sigma/\partial V \\
&\quad + \sum_{\sigma=k_{\rm elem}+2}^{k_{\rm spec}} \mu_\sigma \partial N_{\rm eq}(T,V,\vec{\epsilon},M)_\sigma/\partial V \\
&= \partial F(T,V,\vec{N}_{\rm eq})/\partial V. \qquad (16)
\end{aligned}$$

Similarly,

$$\partial F_{\rm eq}(T,V,\vec{\epsilon},M)/\partial T = \partial F(T,V,\vec{N}_{\rm eq})/\partial T. \qquad (17)$$

These two equations show that to satisfy equation (13) the partial derivative of the free energy with respect to V with $\vec{N}$ constrained to equilibrium values that *vary with* V must be equal to the partial derivative of the free energy with respect to V with $\vec{N}$ constrained to equilibrium values that *are held constant*, and similarly for the partial derivatives with respect to T. Furthermore, equations (6), (7), (8), (16), and (17) imply

$$\begin{aligned}
P_{\rm eq}(T,V,\vec{\epsilon},M) &\equiv P(T,V,\vec{N}_{\rm eq}) \\
&= -\partial F(T,V,\vec{N}_{\rm eq})/\partial V \\
&= -\partial F_{\rm eq}(T,V,\vec{\epsilon},M)/\partial V, \qquad (18)
\end{aligned}$$

$$\begin{aligned}
S_{\rm eq}(T,V,\vec{\epsilon},M) &\equiv S(T,V,\vec{N}_{\rm eq}) \\
&= -\partial F(T,V,\vec{N}_{\rm eq})/\partial T \\
&= -\partial F_{\rm eq}(T,V,\vec{\epsilon},M)/\partial T, \qquad (19)
\end{aligned}$$

and

$$\begin{aligned}
U_{\rm eq}(T,V,\vec{\epsilon},M) &\equiv U(T,V,\vec{N}_{\rm eq}) \\
&= F(T,V,\vec{N}_{\rm eq}) + TS(T,V,\vec{N}_{\rm eq}) \\
&\equiv F_{\rm eq}(T,V,\vec{\epsilon},M) + TS_{\rm eq}(T,V,\vec{\epsilon},M). \qquad (20)
\end{aligned}$$

For fixed chemical composition and mass, equations (18) through (20) show that the relationships between $F_{\rm eq}$, $P_{\rm eq}$, $S_{\rm eq}$, and $U_{\rm eq}$ are identical to the relationships between F, P, S, and U given by equations (6) through (8). Thus, Maxwell's relations are satisfied and thermodynamic consistency prevails not only for arbitrary fixed $\vec{N}$, but also for chemical equilibrium (i.e., when eq. [13] is satisfied) where $\vec{N}$ becomes an implicit function of T, V, $\vec{\epsilon}$, and M. Since the equilibrium constants (see Sect. 4) are derived from equation (13), the FreeEOS implementation automatically provides thermodynamically consistent results limited only by the usual round-off errors expected for double-precision (64-bit word length) floating-point calculations.

4. The Equilibrium Constants

The so-called equilibrium constants that are the basis of the present method of minimizing the free energy are most easily expressed for a free energy model that is divided between known ideal and modelled non-ideal components;

$$F(T,V,\vec{N}) \equiv F^{\mathbf{i}}(T,V,\vec{N}) + F^{\mathbf{ni}}(T,V,\vec{N}). \tag{21}$$

The ideal part of the free energy is made up of a number of known components;

$$F^{\mathbf{i}}(T,V,\vec{N}) \equiv F_R + F_E + F_T + F_L. \tag{22}$$

The ideal free-energy component due to radiation is

$$F_R \equiv -\frac{1}{3}aT^4V, \tag{23}$$

where $a \equiv 4\sigma_{\rm SB}/c$ is the radiation-pressure constant, $\sigma_{\rm SB}$ is the Stefan-Boltzmann constant, and c is the speed of light. This is an important component of the free energy because it strongly affects a number of thermodynamic quantities at low density and high temperature, but it has no effect on equilibrium constants because it is independent of number densities.

The ideal free-energy component due to free electrons is

$$F_E \equiv -P_eV + \eta n_e kTV, \tag{24}$$

where the electron pressure is P_e, the electron number density is $n_e \equiv N_e/V$, and η is a well-known degeneracy parameter (see, e.g., eqs. [24.98] through [24.100] of Cox & Giuli 1968). All other components of $F^{\mathbf{i}}$ are independent of N_e. Thus, from equations (22) and (24) and the thermodynamic relationship,

$$n_e = \frac{1}{kT}\frac{P_e(\eta,\beta)}{\partial\eta} \tag{25}$$

(see eq. [25] of Paper I), it directly follows that

$$\mu_e^{\mathbf{i}} \equiv \partial F^{\mathbf{i}}(T,V,\vec{N})/\partial N_e = \partial F_E(T,V,N_e)/\partial N_e = kT\eta. \tag{26}$$

Because the approximations for P_e and n_e (see Paper I) used in the FreeEOS implementation are designed to be thermodynamically consistent with each other, equations (25) and (26) hold exactly in that implementation limited only by the usual round-off errors expected for double-precision floating-point calculations.

The ideal free-energy component due to translational degrees of freedom of non-electron species is

$$F_T = -kTV\sum_{\sigma\neq e} n_\sigma[1 - \ln(n_\sigma) + \ln(q_\sigma^T)], \tag{27}$$

where σ indexes the chemical species other than the free electron, $n_\sigma \equiv N_\sigma/V$ is the number density,

$$q_\sigma^T = {\lambda_\sigma}^{-3} \exp(-c_2 E_{1\sigma}/T) \tag{28}$$

is the translational partition function per unit volume,

$$\lambda_\sigma = (2\pi m_\sigma kT/h^2)^{-1/2} \tag{29}$$

is the de Broglie wavelength, m_σ is the mass, $E_{1\sigma}$ is the ground state energy (with units of inverse wavelength), and $c_2 \equiv hc/k$ is the second radiation constant.

The ideal free-energy component due to internal degrees of freedom of lower energy levels of non-electron species is

$$F_L = -kTV \sum_{\sigma \neq e} n_\sigma \ln(Q_\sigma^L), \tag{30}$$

where

$$Q_\sigma^L = \sum_{i=1} g_{i\sigma} \exp[-c_2(E_{i\sigma} - E_{1\sigma})/T] \tag{31}$$

is the ideal internal partition function of the lower energy levels with $g_{i\sigma}$ the statistical weight, and $E_{i\sigma}$ the energy of the ith level. The lower energy levels include at least the ground state and any additional levels that are too low in energy to be well-approximated by the Rydberg formula. The non-ideal corrections to the effect of the lower energy levels and the entirety of the effect of the Rydberg energy levels on the free energy depend on the adopted model for $F^{\mathbf{ni}}$.

All components of $F^{\mathbf{i}}$ other than F_T and F_L are independent of N_σ. Thus, equations (22), (27), and (30) imply the ideal chemical potential for non-electron species is

$$\mu_\sigma^{\mathbf{i}} \equiv \partial F^{\mathbf{i}}(T, V, \vec{N})/\partial N_\sigma = [F_T(T, V, \vec{N}) + F_L(T, V, \vec{N})]/\partial N_\sigma = kT[\ln(n_\sigma) - \ln(q_\sigma^T Q_\sigma^L)]. \tag{32}$$

Equation (13) is a necessary condition that chemical equilibrium has been obtained and the free energy has been minimized. Combination of that result with equations (26) and (32) yields

$$\ln n_\sigma = \ln K_\sigma + \sum_{j=1}^{k_{\mathrm{elem}}} C_{\sigma j} \ln n_j \tag{33}$$

for $\sigma = k_{\mathrm{elem}} + 2, \ldots, k_{\mathrm{spec}}$, where the equilibrium constant is

$$\ln K_\sigma = \ln(q_\sigma^T Q_\sigma^L) - \sum_{j=1}^{k_{\mathrm{elem}}} C_{\sigma j} \ln(q_j^T Q_j^L) + C_{\sigma e}\, \eta + \Delta \ln K_\sigma, \tag{34}$$

its non-ideal correction is

$$\Delta \ln K_\sigma = -\left(\mu_\sigma^{\mathbf{ni}} - \sum_{j=1}^{k_{\mathrm{elem}}+1} C_{\sigma j} \mu_j^{\mathbf{ni}} \right) /(kT), \tag{35}$$

and the non-ideal components of the chemical potential are (for $k = 1, \ldots, k_{\rm spec}$)

$$\mu_k^{\mathbf{ni}} \equiv \partial F^{\mathbf{ni}}(T, V, \vec{N})/\partial N_k. \tag{36}$$

Equation (33) constitutes the fundamental relationship between the number density of non-reference species, associated equilibrium constants, and the number density of reference species that is the basis (see Sect. 6) for the solution of the EOS in the FreeEOS implementation. This equation is equivalent to both the Saha ionization equation for ions and dissociation equation for molecules corrected in a thermodynamically consistent way for non-ideal effects. Thus, it also can be adopted as the basis of the EOS calculation used for physical conditions in stellar atmospheres, e.g., the EOS calculation in the synthetic spectrum application, SSynth (http://sourceforge.net/projects/ssynth).

5. Auxiliary Variables

Section 6 shows that the EOS solution follows directly from equations (4) and (33); the equilibrium constants as defined by equation (34); and the fundamental independent variables of the FreeEOS calculation which are f, T, and $\vec{\epsilon}$. For example, the degeneracy parameter η that appears in equation (34) is defined by

$$\eta \equiv \ln f + 2\left[\sqrt{1+f} - \ln\left(1 + \sqrt{1+f}\right)\right]. \tag{37}$$

Furthermore, the number density of elections n_e that appears in the charge neutrality equation is approximated in a thermodynamically consistent way (see Paper I) as a function of f and g, where

$$g \equiv \beta\sqrt{1+f} \equiv \frac{kT}{m_e c^2}\sqrt{1+f}. \tag{38}$$

The equilibrium constants that are required by the EOS solution depend on physical data, T, and $\Delta \ln \vec{K}$. Furthermore, $\Delta \ln \vec{K}$ depends (in general) on physical data, f, T, and a set of auxiliary variables which depend on the adopted model for $F^{\mathbf{ni}}$. For example, if the FreeEOS implementation of the Coulomb effect is included in $F^{\mathbf{ni}}$, $\Delta \ln \vec{K}$ depends (in part) on the two auxiliary variables,

$$\Sigma_0^C \equiv \sum_{\Pi} n_\Pi \tag{39}$$

and

$$\Sigma_2^C \equiv \sum_{\Pi} n_\Pi {Z_\Pi}^2, \tag{40}$$

where the Π index ranges over all positive ions, and Z_Π is the charge of the ion. I have programmed a large choice of components for $F^{\mathbf{ni}}$ in the FreeEOS implementation, and later papers in this series will give implementation details of each component (such as the Coulomb effect) as well as the associated auxiliary variables. In general, as in the two example auxiliary variables above,

auxiliary variables depend on the individual species number densities which depend in turn on the solution of the EOS. Thus, an iterative procedure (Sect. 6) must be used to determine the auxiliary variables.

Fortunately, the user of the FreeEOS code does not have to worry about any of these specifics because I have been able to design the code so that the number and definition of the auxiliary variables is automatically selected depending on the chosen option suite. It turns out that the number of required auxiliary variables ranges from none for the "PTEH" option suite that mimics the Pols et al. 1995 (hereafter, PTEH) non-ideal free-energy model to 15 for the "EOS1" option suite (described in Paper I) that is specially designed to fit the detailed OPAL results (Rogers & Nayfonov 2002, hereafter EOS2001).

6. Solution of the EOS

For the case where the equilibrium constants are independent of auxiliary variables, the solution of the EOS is straightforward. n_e is already known in terms of the independent variables of the FreeEOS implementation. Thus, substitution of the equilibrium relations (eq. [33]) into the abundance conservation and charge neutrality constraint equation (eq. [4]) results in $k_{\rm elem}$ equations to be solved for the $k_{\rm elem}$ unknowns $\vec{n}^{\mathbf{r}}/\rho$, where $\vec{n}^{\mathbf{r}}$ is the number density of reference species and $\rho \equiv M/V$ is the mass density. For the physical conditions found in cool stellar atmospheres, the EOS solution is complicated by cross-terms between the equations which are caused by heteronuclear molecules such as CO. However, for stellar-interior conditions this aspect of the EOS greatly simplifies. At temperatures above 10^6 K the FreeEOS implementation ignores molecular formation altogether. In this case, $\vec{n}^{\mathbf{r}}/\rho$ can be directly obtained from the abundance conservation constraint equations with the required number of floating-point operations proportional to $k_{\rm spec}$. ρ is then found from the charge neutrality constraint equation. This gives $\vec{n}^{\mathbf{r}}$ and (via the equilibrium constants and eq. [33]) $\vec{n}^{\mathbf{nr}}$, the number density of non-reference species. Knowledge of $\vec{n}^{\mathbf{r}}$ and $\vec{n}^{\mathbf{nr}}$determines the remainder of the EOS solution. First and second partial derivatives of the free energy are evaluated to machine precision using analytical expressions derived from the chain rule, and first- and second-order thermodynamic functions can be obtained starting with the definitions given by equations (18) through (20).

At temperatures below 10^6 K the solution of the present EOS is only slightly more complicated. The FreeEOS implementation uses the approximation that all molecules can be ignored except for H_2 and H_2^+. In this case, it is possible to formally solve the hydrogen number constraint equation (eq. [1]) for

$$\rho = \{2[K(H_2^+) + K(H_2)]n(H)^2 + [1 + K(H^+)]n(H)\}/[N_0\epsilon(H)]. \quad (41)$$

Substitution of this result into the charge neutrality equation gives a quadratic equation in $n(H)$,

$$\{K(H_2^+) + 2[K(H_2^+) + K(H_2)]\Sigma^+\}n(H)^2 + \{K(H^+) + [1 + K(H^+)]\Sigma^+\}n(H) = n_e, \quad (42)$$

where

$$\Sigma^+ = \sum_\sigma n_\sigma Z_\sigma / [\rho N_0 \epsilon(\mathrm{H})], \tag{43}$$

and the sum is to be taken over all non-hydrogen positive ions. This sum can be determined from abundance conservation constraint equations for each element similar to equation (2). Once the solution of the quadratic has been obtained, the density can be determined from equation (41) and all remaining reference number densities can be obtained from the abundance conservation constraint equations. The remaining steps to determine the first- and second-order thermodynamic functions follow the procedure discussed above for the no-molecules case.

So far, I have discussed only the case where the equilibrium constants are independent of auxiliary variables. If the equilibrium constants do depend on auxiliary variables, then the EOS solution is more complicated. Given an "input" set of auxiliary variables the EOS solution proceeds as before including a calculation of all number densities. These in turn are used to calculate an "output" set of auxiliary variables, and iteration is required to achieve consistency between the two sets of auxiliary variables. Typically, for stellar models or EOS table generation, physical conditions do not change very much between successive calculations of the EOS. Under these conditions the previous solution of the EOS provides a Taylor series approximation for the initial values of the auxiliary variables for the next solution of the EOS. However, if the physical conditions have changed too much or if it is the first call of the FreeEOS routine, the implementation makes a preliminary solution that uses the PTEH form of free-energy model. This preliminary EOS can be solved without auxiliary-variable iteration and the results used to make preliminary estimates of the auxiliary variables associated with the required free-energy model. The FreeEOS implementation employs a Newton-Raphson procedure to iterate the auxiliary variables to consistency. The Jacobian calculation requires the inner product of the partial derivatives of the output auxiliary variables with respect to the equilibrium constants and the partial derivatives of the equilibrium constants with respect to the input auxiliary variables. Thus, the required number of floating-point calculations per iteration is roughly proportional to $k_{\mathrm{eq}} k_{\mathrm{aux}}^2$, where $k_{\mathrm{eq}} \equiv (k_{\mathrm{spec}} - k_{\mathrm{elem}} - 1)$ is the number of equilibrium constants and k_{aux} is the number of auxiliary variables. Once the Newton-Raphson iteration to determine the auxiliary variables has converged, the remaining steps to determine the first- and second-order thermodynamic functions follow the procedure discussed for the case where no auxiliary variables need to be determined except that certain of the required derivatives are determined using the chain rule and the Jacobian of the linear system of equations evaluated for the converged Newton-Raphson solution.

So far, I have assumed in the discussion that the user has specified f, T, and $\vec{\epsilon}$, the fundamental independent variables of FreeEOS. However, the FreeEOS user also has the option of selecting a different set of independent variables where f is replaced in the set by a "match" variable which is either P, P_{gas}, or ρ. Such options are implemented by an "outer" Newton-Raphson iteration to find the f value that is consistent with the match variable, and the previously described "inner" Newton-Raphson iteration to find a self-consistent set of auxiliary variables. The termination algorithm used for both iterations is to perform one additional iteration beyond where agreement is obtained

to 1 part in 10^7. Because of the quadratic convergence of the Newton-Raphson technique, this algorithm should ideally yield numerical precision of order 1 part in 10^{14}, but the actual numerical precision obtained (see Sect. 7.1) can be somewhat worse than this because of numerical significance loss.

7. Results and Discussion

To give the following results and discussion some context, Figure 1 shows the loci of several stellar interior models on the density-temperature plane. The high-density, low-temperature region bounded by the diagonal jagged line on the left, and the $\log T = 6$ isotherm at the top is excluded for all FreeEOS computations for the reasons discussed in Section 7.4.

7.1. Numerical Quality of Results

The FreeEOS implementation of the above equilibrium-constant technique for minimizing the free energy requires knowledge of large numbers of analytical first and second partial derivatives of the modelled free-energy expression. I have comprehensively checked (with the free_eos_test application that is documented at http://freeeos.sourceforge.net/documentation.html) the derivation and programming of these required analytical derivatives by comparing with centred numerical differences with optimal step sizes. As expected for such differences, the size of the disagreement with analytical derivatives is proportional to the square of the step size for large step sizes and for small step size, where significance loss in the differences becomes an important factor, the disagreement is proportional to the inverse of the step size. By varying the step size in a systematic way, one can find the optimal intermediate step size where the centred difference approach yields the most error-free (typically with relative errors of 1 part in 10^9 for double-precision calculations) comparisons with the analytical derivatives. Indeed, comparing with numerical differences this way has proved to be a powerful tool for removing all errors (to this level) in the derivation or programming of the partial derivatives in the FreeEOS implementation because such errors give a characteristic signature of a constant difference with numerical difference results over a range of different step sizes near the optimal value.

A further measure of the numerical quality of the FreeEOS implementation can be obtained by comparing results calculated on different Fortran/hardware platforms. Different Fortran compilers (or even different degrees of optimization for the same compiler) do floating-point calculations in a variety of orders. Furthermore, different hardware platforms have different floating-point representations and different procedures for rounding results. The result is that rounding errors propagate in quite different ways on different Fortran/hardware platforms for the same Fortran source code, and these cross-platform differences are a measure of the typical amount of rounding error propagation for the code. The stable releases of the FreeEOS source code (see http://freeeos.sourceforge.net/)

have been compiled by users for a wide variety of Fortran/hardware platforms, and the reported test results are typically consistent to 1 part in 10^{12} or better. That is satisfactory numerical quality for an EOS calculation that necessarily requires a large number of double-precision floating-point calculations (with associated propagation of numerical errors) to obtain results.

The good agreement between the analytical partial derivatives and corresponding numerical differences and the good agreement between results for various platforms are both indications of the high degree of numerical quality of the FreeEOS results for the free-energy models that have been implemented. Nevertheless, I emphasize that the actual errors in the FreeEOS results compared to physical reality depends very much on the realism of the free-energy model that is being used (see discussion in Sect. 7.4), and in general those actual errors are much larger than the numerical errors I have been discussing in this subsection.

7.2. Thermodynamic Consistency

As an additional check of the thermodynamic consistency and numerical quality of the FreeEOS results, I have evaluated the thermodynamic inconsistency index,

$$\alpha \equiv \ln \left\{ \frac{\partial s(\rho, T, \vec{\epsilon})}{\partial \rho} \left[\frac{\partial \rho(P, T, \vec{\epsilon})/\partial T}{\rho^2 \partial \rho(P, T, \vec{\epsilon})/\partial P} \right]^{-1} \right\}, \tag{44}$$

where $s(\rho, T, \vec{\epsilon})$ is the entropy per unit mass in chemical equilibrium.

Equations (18) through (20) satisfy Maxwell's relations at chemical equilibrium so that α should be zero for error-free EOS calculations done with the equilibrium-constant approach that have been converged to exact chemical equilibrium. In actual calculations α will differ from zero if the relevant analytical derivatives are improperly derived or programmed or there is some other inconsistency with the modelled free-energy.

For example, Figure 2 illustrates the systematic variations of α from zero caused by approximating the Fermi-Dirac integrals using thermodynamically consistent coefficients that are rounded to six figures beyond the decimal like the coefficients published in Table 5 of Eggleton, Faulkner, & Flannery (1973, hereafter EFF) and Table A1 of PTEH. The rounding causes little inconsistency at high temperatures and low densities because radiation dominates the free-energy model there, and at low temperatures because ionization is low and electrons are not important. However, the rounding of the coefficients does have a discernible effect where electrons are important. Even in those regions, the thermodynamic inconsistency caused by this small degree of rounding is actually perfectly acceptable, but I like to remove it to make sure there are no other more subtle sources of inconsistencies. Such removal is straightforward; the FreeEOS normally (except for the special rounded case shown in Fig. 2) uses the relations in Paper I to calculate the thermodynamically consistent coefficients to the numerical precision allowed by double-precision floating-point calculations. Such calculations may be based on the original $\widehat{P}_{nm}$ coefficients of Table 3 of EFF, or, better

yet, the improved $\widehat{P}_{nm}$ coefficients taken from Table 1 of Paper I. The substantially improved thermodynamic consistency that results from removing the rounding is obvious in the comparison between Figures 2 and 3, and I ascribe the remaining non-systematic deviations of α from zero to numerical noise in the FreeEOS calculation.

The high degree of thermodynamic consistency normally exhibited by the FreeEOS implementation is a useful indication that the programmed analytical derivatives and all other aspects of the implementation are consistent with the adopted free energy model to roughly 1 part in 10^{11} or better. That level of numerical inconsistency is satisfactory for an EOS calculation which necessarily has many double-precision floating-point calculations (with associated propagation of numerical errors) and is another indication of the high numerical quality of FreeEOS results. Nevertheless, a similar remark applies here as in Section 7.1; the physical realism of the free-energy model determines the actual errors of the FreeEOS results compared to physical reality, and those actual errors (see Sect. 7.4) are much larger than the minute degree of thermodynamic inconsistency exhibited in Figure 3.

7.3. FreeEOS Computation Efficiency

The most realistic (and complex) "EOS1" option suite for FreeEOS has 15 associated auxiliary variables. Since that number is much smaller than the typical number of variables being iterated in a traditional free-energy minimization for realistic abundance mixtures, a FreeEOS calculation is quite efficient compared to other free-energy minimization procedures. For example, a typical FreeEOS computation with the 'EOS1" option suite and mixture of 20 elements in the abundance mix only requires 0.01 sec to complete on a 600MHz PC.

7.4. Validity of the FreeEOS Results

To give some context to the following discussion of the validity of FreeEOS results, refer back to Figure 1 which shows the loci of several stellar interior models on the density-temperature plane. The strength of interactions between particles increases as the mean distance between particles decreases or the density increases. Also, at lower temperature the particles are less ionized and therefore larger so that the so-called "pressure-ionization effects" which are difficult to model reliably and which account for deviations from a model of interacting point charges become more important. The net result is EOS calculations tend to be the least reliable for extreme lower main-sequence envelope conditions such as those that occur in the 0.1-$M_\odot$ model in the figure, and the free-energy models available for FreeEOS are no exceptions to this general rule.

The OPAL EOS2001 results give reasonable agreement with the observed solar Γ_1 values determined as a function of radial distance from the solar centre by inversion techniques but, like other equations of state, are expected to have substantially larger errors for extreme lower main sequence

envelope conditions (EOS2001). Nevertheless, EOS2001 results are probably the best available, and therefore, the realism of the various free-energy models available for FreeEOS is judged by how closely the FreeEOS results match those from the EOS2001 tabulations. (EOS2001 results required a supercomputer to calculate so are only available in tabular form with the associated inherent concerns about interpolation errors [Dorman, Irwin, & Pedersen 1991] and the fixed and truncated abundance mixes.)

The EOS1 option suite gives the most realistic free-energy model currently programmed for FreeEOS. This free-energy model has many components included in it (see summary in Paper I) specifically designed to yield the best agreement with tabulated (not interpolated) EOS2001 results when the EOS2001 abundance mix is used for the FreeEOS calculation. Good preliminary results have already been obtained in comparison to EOS2001 for solar conditions (see Sect. 7.4.1). However, the EOS1 free-energy model for pressure ionization currently just uses a hard-sphere potential following the MDH work, and because of this limitation there are islands in the density-temperature plane at high densities and low temperatures characteristic of the physical conditions of extremely low-mass stars where the FreeEOS calculation with EOS1 option suite fails to converge, or gives non-physical results.

To completely avoid these problem areas for the FreeEOS results reported in the remainder of this paper, I have imposed a calculation limit for $\log T < 6$ of

$$\log \rho_{\rm lim} = \log \rho_5 + (3/2) \log(T/10^5), \tag{45}$$

for $\log \rho_5 = 3.3$. (Note all units in this paper are SI unless specifically stated otherwise.) The actual limit used for this paper is quantized (see Fig. 1) by the $\log \rho$ and $\log T$ step sizes used for the EOS tabulations for the later figures in this paper. (Note the FreeEOS implementation is fast enough to be called directly from a stellar-interior code so pre-computed tables of results are not necessary in that case.) This calculation limit roughly corresponds to a 0.1-$M_\odot$ model and can also be viewed as the approximate limit of validity for FreeEOS calculations with the EOS1 option suite. However, this limit is just a preliminary result, and for the next release of FreeEOS, I plan to make some pressure-ionization adjustments to see if it is possible to push the EOS1 calculational limit slightly higher than $\log \rho_5 = 3.3$ which would allow models at the main-sequence hydrogen-burning limit near 0.07 $M_\odot$ to be calculated with the EOS1 option suite of FreeEOS.

7.4.1. Comparison of FreeEOS and OPAL results for a Solar Model

I compare FreeEOS results with two distinct sets of OPAL calculations for the solar case. I use the term "EOS1995" to designate the older set of OPAL calculations. Rogers, Swenson, and Iglesias (1996) describe these calculations, and the results are stored in files named Neos... that are currently accessible at ftp://www-phys.llnl.gov/pub/opal/eos. The "readme" file at that location indicates the last update of these tables was in 1995, hence their designation. I have previously used the term "EOS2001" to designate the modern set of OPAL calculations. The EOS2001 reference

describes these calculations, and the results are stored in files named IEOS... that are currently accessible at http://www-phys.llnl.gov/Research/OPAL/Download/. The EOS2001 reference discusses the improvements between the EOS1995 and EOS2001 calculations; these primarily concern the electron treatment (done relativistically for the first time in EOS2001) and the molecular treatment.

Figure 4 shows the comparison between solar results for EOS1995 and EOS2001. No interpolation is used in the comparison. Instead, for each (ρ, T) point in a solar-interior model, the nearest common (ρ, T) point is selected from the OPAL EOS1995 and EOS2001 tables, and thermodynamic quantities directly compared (with residuals taken in the sense of EOS1995 minus EOS2001). For these figures the comparisons were made between the ($X = 0.6$, $Y = 0.38$, and $Z = 0.02$) EOS1995 and EOS2001 tables, but results tabulated for EOS1995 and EOS2001 for other abundances show similar differences as well.

The $\Delta\Gamma_1$ result from Figure 4 is similar to Figure 8 of the EOS2001 reference for $r/R < 0.95$. For this region of the model almost all the differences between the two OPAL calculations are due to the improved relativistic treatment of electrons in the EOS2001 calculation. However, note the $\Delta\Gamma_1$ residuals from Figure 8 of the EOS2001 reference for $r/R > 0.95$ are an order of magnitude smaller than the corresponding residuals in Figure 4. I have no explanation for this discrepancy. I believe the present comparisons between EOS1995 and EOS2001 for the solar case are reliable since I have directly confirmed that the present plots reflect the actual EOS1995 and EOS2001 tables.

Figure 5 is identical to Figure 4 except that the independent variable is $\log T(r)$ rather than r/R. This way of plotting the residuals shows more details for the outer region of the model. (Comparison of the two figures shows $r/R = 0.95$ roughly corresponds to $\log T(r) \simeq 5.4$.) Clearly, for $\log T(r) < 5.4$ there are substantial (by the standards of helioseismology) differences between the two generations of OPAL calculations. These difference are a surprise, however, since in this region both molecular formation and relativistic corrections are negligible, and the known changes in the treatment of these two effects between the EOS1995 and EOS2001 calculations cannot be the cause of these discrepancies. Therefore, I feel it is important for the OPAL team to investigate these differences between their two results more thoroughly.

The pressure-ionization model used for the EOS1 option suite for FreeEOS, has coefficients (the interaction radii which characterize the MDH-like occupation probability formalism) that can be adjusted to fit more detailed calculations. For FreeEOS–1.1.0, the latest released version of the code, these coefficients have been adjusted to give a good fit of EOS1995 results from OPAL, an extension (Rogers 1995) of those results to high densities and low temperatures using the same code that produced the EOS1995 results, and EOS results from Saumon, Chabrier, & Van Horn (1995). The "EOS1995" option-suite used for the FreeEOS–1.1.0 comparison with EOS1995 results is identical to the EOS1 option suite except for the following changes that were introduced to mimic known deficiencies in the EOS1995 calculation: H_2^+ was ignored, all levels with principal quantum number greater than 4 were ignored, and relativistic corrections were ignored. (The last of these

changes is the most important one for solar conditions.) Also, as a matter of convenience the well-known radiation terms are dropped from the FreeEOS EOS1995 option suite rather than added to the OPAL EOS1995 tabulated results. Figure 6 shows the resulting small residuals between FreeEOS(EOS1995) and EOS1995 for the solar case. Particularly noteworthy is the maximum residual of 0.0006 in $\ln P$ which is more than 5 times smaller than the maximum residual in $\ln P$ between EOS1995 and EOS2001 shown in Figure 5.

Compared to EOS1995, the EOS2001 calculations extend to much higher densities at low temperatures (in fact almost to the conditions appropriate for a 0.1-$M_\odot$ model). Thus, my plan for the next release of the FreeEOS code is to adjust the pressure-ionization coefficients of the EOS1 option suite to fit the EOS2001 results throughout its tabulated density, temperature, and abundance range.

Such a preliminary adjustment has already been made. The resulting pressure-ionization coefficients are quite different than those used for the EOS1 (and EOS1995) option suites of FreeEOS–1.1.0, and there is a small but noticeable change in the solar comparisons below $\log T = 5.4$ as a result. In addition for the solar comparison with EOS2001, the full EOS1 option suite has been used (except for radiation). In particular, H_2^+ (whose treatment will be described in a future paper in this series), principal quantum numbers up to 100, and relativistic corrections are all included. Figure 7 shows the resulting residuals between FreeEOS(EOS1) (with updated pressure-ionization coefficients) and EOS2001 in the solar case. For $\log T > 5.4$ (or $r/R < 0.95$) the residuals are extremely small just as for the comparison with EOS1995 in Figure 6. In other words, the relativistic correction that has always been a part of the EOS1 option suite is now well-matched by the EOS2001 calculation. However, for $\log T < 5.4$ the changes in pressure-ionization coefficients that have been made since FreeEOS–1.1.0 was released are not sufficient to completely overcome the differences between EOS1995 and EOS2001. For example, the maximum $\ln P$ residual in Figure 7 is half that in Figure 5 but 2.5 times that in Figure 6. An explanation of why the EOS2001 result differs from the EOS1995 result for this region should help improve the free-energy model used by the FreeEOS EOS1 option suite.

8. Conclusions

Because only a relatively small number of auxiliary variables need to be iterated to convergence, the equilibrium-constant approach for minimizing the free energy is so efficient it can easily be calculated on a low-end PC. (The FreeEOS code was originally developed on a Pentium-133.) Also, results from the technique have high numerical quality, and this is also reflected in the large degree of thermodynamic consistency of the results as seen in Figure 3. Therefore I recommend consideration of the equilibrium-constant approach for all future EOS implementations that use the free-energy minimization technique.

The "EOS1" suite of options currently gives the most realistic free-energy model that I

have programmed as part of the FreeEOS implementation. Figure 7 shows that differences of FreeEOS(EOS1) and EOS2001 thermodynamic quantities for the solar case are generally smaller than the corresponding differences between the EOS1995 and EOS2001 OPAL results (shown in Fig. 5) and differences between thermodynamic functions derived with inversion of helioseismology data and EOS2001 OPAL results (e.g., Fig. 8 of the EOS2001 reference). Thus, FreeEOS(EOS1) has a similar degree of realism as EOS2001 at least in the solar case. Furthermore, FreeEOS provides an ideal EOS platform that for a wide range of physical conditions can be used to explore numerical effects such as interpolation errors as well as physical effects such as changes in the adopted abundance mix or free-energy model.

The FreeEOS software is licensed under the GPL and is freely downloadable from http://freeeos.sourceforge.net/. Two stable releases of the source code have already been made, and another one is planned for the near future. Further papers in this series describing the FreeEOS implementation are planned including details of the large variety of free-energy models that are currently available with the FreeEOS implementation.

I thank Forrest Rogers for many useful discussions and for providing unpublished data; Ben Dorman and Fritz Swenson for helping to arouse my original interest in the EOS problem for stellar interiors; Don VandenBerg for providing some representative model calculations using a preliminary version of the FreeEOS code; and Richard Stallman, Linus Torvalds, and many other programmers for the GNU/Linux computer operating system and accompanying tools that have made it practical to develop the FreeEOS code. The figures of this paper have been generated with the yPlot (http://yplot.sourceforge.net) and PLplot (http://www.plplot.org) scientific plotting packages.

REFERENCES

Cox, J.P. & Giuli, R.T. 1968, Principles of Stellar Structure (New York: Gordon and Breach)

Dorman, B., Irwin, A.W., & Pedersen, B.B. 1991, ApJ, 381, 228

Eggleton, P.P., Faulkner, J., & Flannery B.P. 1973, A&A, 23, 325 (EFF)

Irwin, A.W. 2004, http://freeeos.sourceforge.net/eff_fit.pdf (Paper I)

Mihalas, D., Däppen, W., & Hummer, D.G. 1988, ApJ, 331, 815 (MDH)

Pols, O.R., Tout, C.A., Eggleton, P.P., & Han, Z. 1995, MNRAS, 274, 964 (PTEH)

Rogers, F.J. 1995, private communication

Rogers, F.J. & Nayfonov, A. 2002, ApJ, 576, 1064 (EOS2001)

Rogers, F.J., Swenson, F.J., & Iglesias, C.A. 1996, ApJ, 456, 902 (EOS1995)

Saumon, D., Chabrier, G., & van Horn, H.M. 1995, ApJS, 99, 713

VandenBerg, D.A. 1998, private communication

Fig. 1.— A comparison of loci of model stellar interiors calculated for solar metallicity. The models (VandenBerg 1998) were calculated using the University of Victoria stellar-evolution code and a preliminary version of the EOS1 option suite of FreeEOS. The model loci are indicated by thick solid lines labelled by '0.1", '0.3", '1.0", 'RGT", and 'CG" to label respectively main sequence models of 0.1, 0.3, and 1.0 $M_\odot$ and models of 1.0 $M_\odot$ evolved to the tip of the red-giant branch and to the initial clump-giant phase (zero-age horizontal branch of solar metallicity). Note the jagged thin diagonal line near the 0.1-$M_\odot$ model continued by the thin horizontal line at $\log T = 6$ corresponds to the current high-density, low-temperature calculational limit of the EOS1 option suite for FreeEOS (see discussion in Sect. 7.4).

Fig. 2.— The thermodynamic inconsistency index α (eq. [44]) as a function of density and temperature for a special case where I have deliberately introduced small rounding inconsistencies with the free-energy model (see text). The calculated values of α are quite sensitive to such inconsistencies when they exist. Note the α surface is undefined beyond the calculational limit indicated in Figure 1. (See also discussion of this calculational limit in Sect. 7.4.)

Fig. 3.— The thermodynamic inconsistency index α (eq. [44]) as a function of density and temperature for the typical case where there are no known inconsistencies between the programming and free-energy model. Note the α surface is undefined beyond the calculational limit indicated in Figure 1. (See also discussion of this calculational limit in Sect. 7.4.)

Fig. 4.— A comparison of OPAL EOS1995 and EOS2001 results for the solar case. $\Gamma_1 \equiv \partial \ln P(\rho, s)/\ln \rho$, where s is the entropy per unit mass. The adiabatic sound speed is $v_s^2 \equiv \Gamma_1 P/\rho$. The adiabatic temperature gradient is $\nabla_a \equiv (\Gamma_2 - 1)/\Gamma_2 \equiv \partial \ln T(P, s)/\partial \ln P$. See text for details of the tabular comparison.

Fig. 5.— Identical to Figure 4 except that the data are plotted as a function of $\log T(r)$.

Fig. 6.— Identical to Figure 5 except that the comparison is between FreeEOS(EOS1995) (where the EOS1995 option suite of FreeEOS has been optimized for the comparison, see text) and the EOS1995 tabulated results.

Fig. 7.— Identical to Figure 6 except that the comparison is between FreeEOS(EOS1) (with pressure-ionization coefficients updated to get a better fit of EOS2001, see text) and EOS2001 tabulated results.

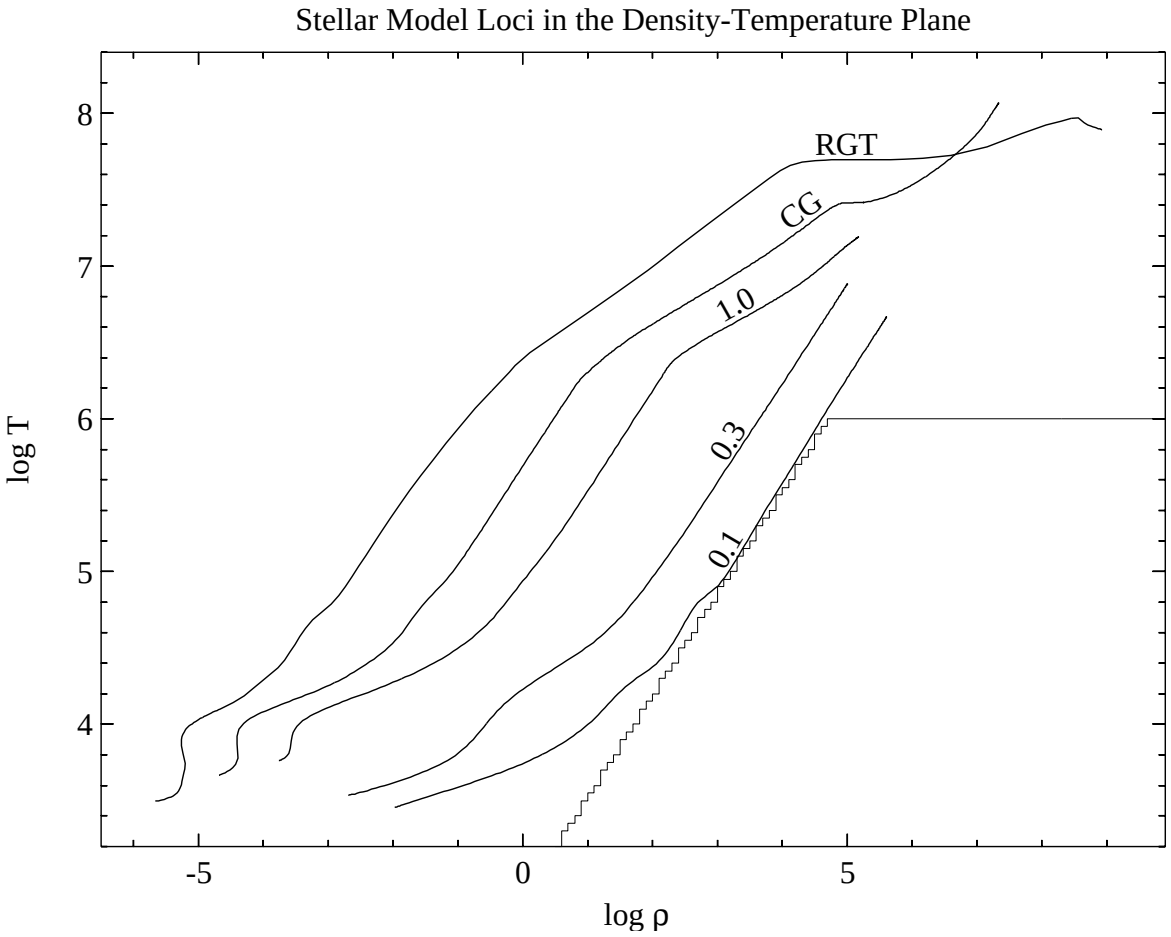
Stellar Model Loci in the Density-Temperature Plane
RGT
CG
1.0
0.3
0.1
log T
log ρ
8
7
6
5
4
-5
0
5

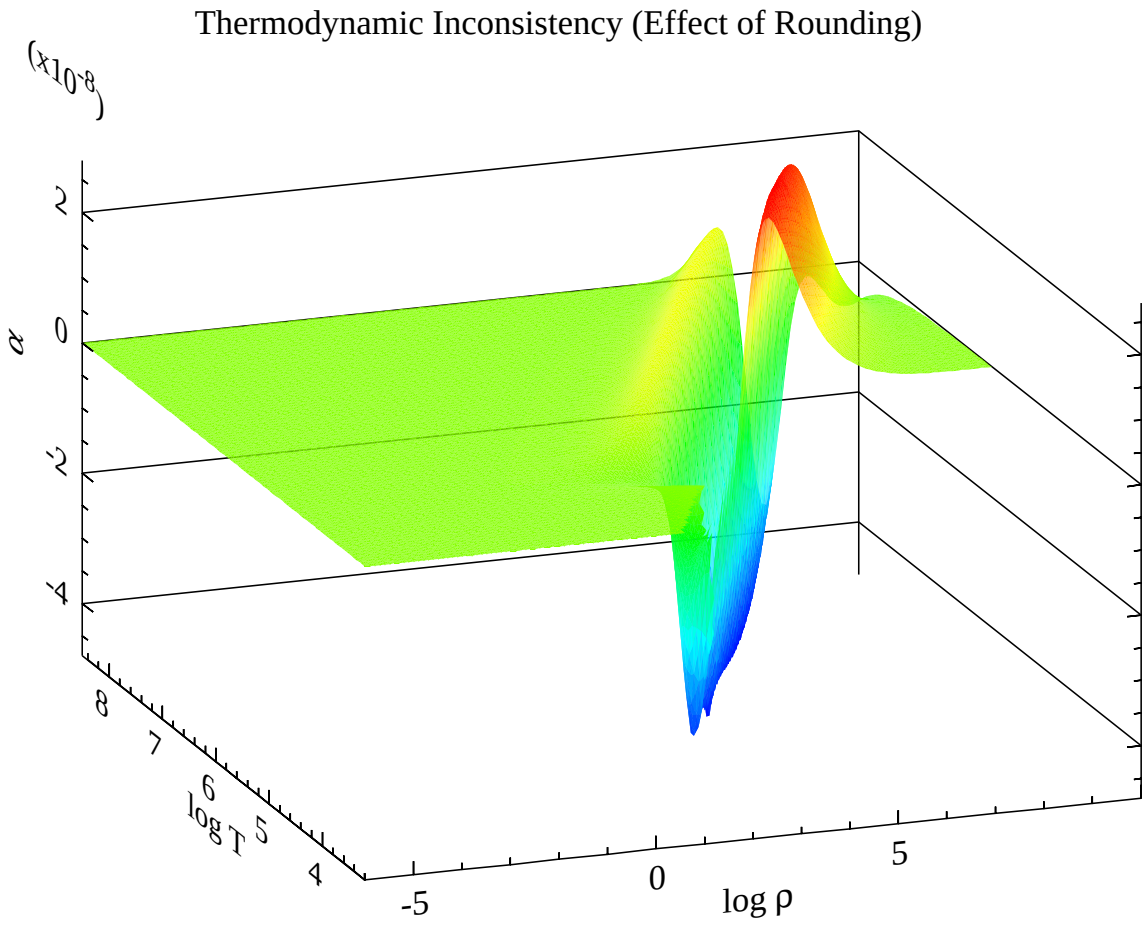
Thermodynamic Inconsistency (Effect of Rounding)
(x10^-8)
2
0
-2
-4
α
8
7
6
log T
5
4
-5
0
5
log ρ

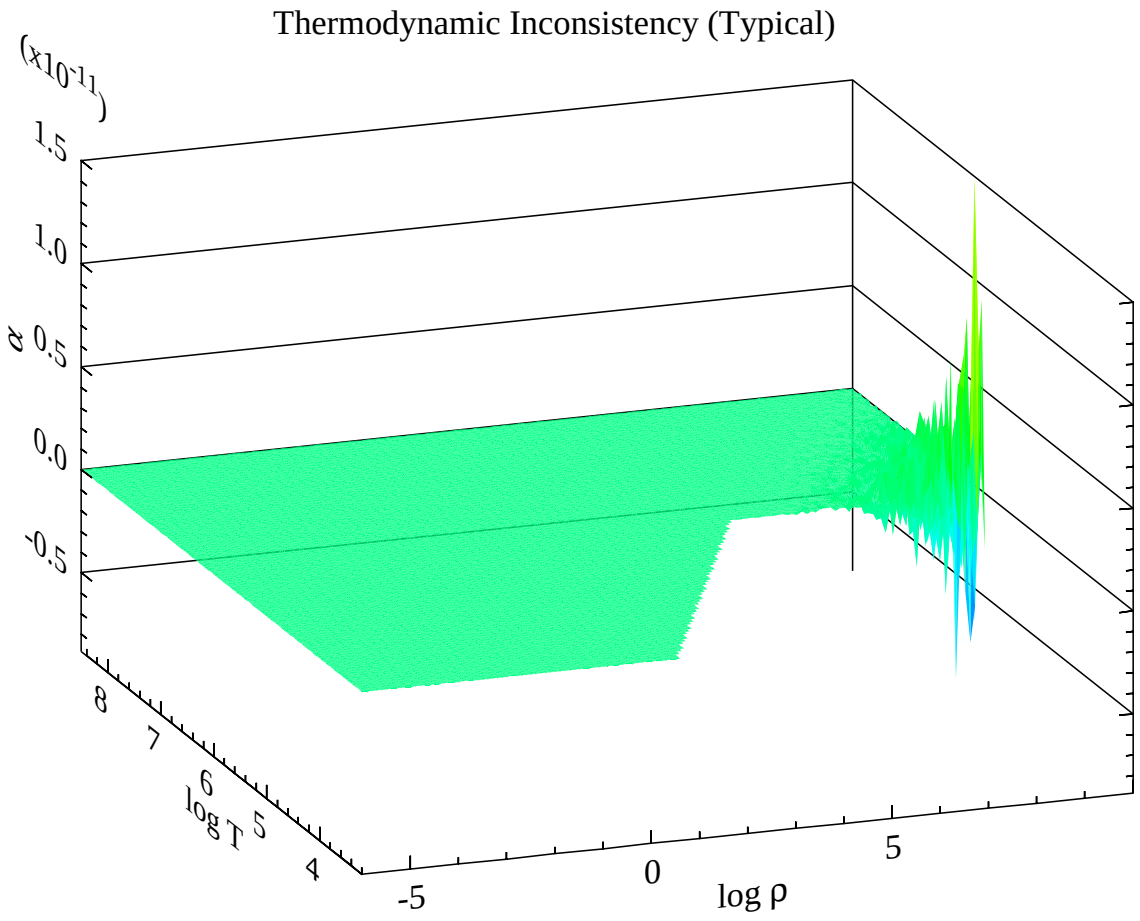
Thermodynamic Inconsistency (Typical)
(x10^-11)
1.5
1.0
0.5
0.0
-0.5
α
8
7
6
5
4
log T
-5
0
5
log ρ

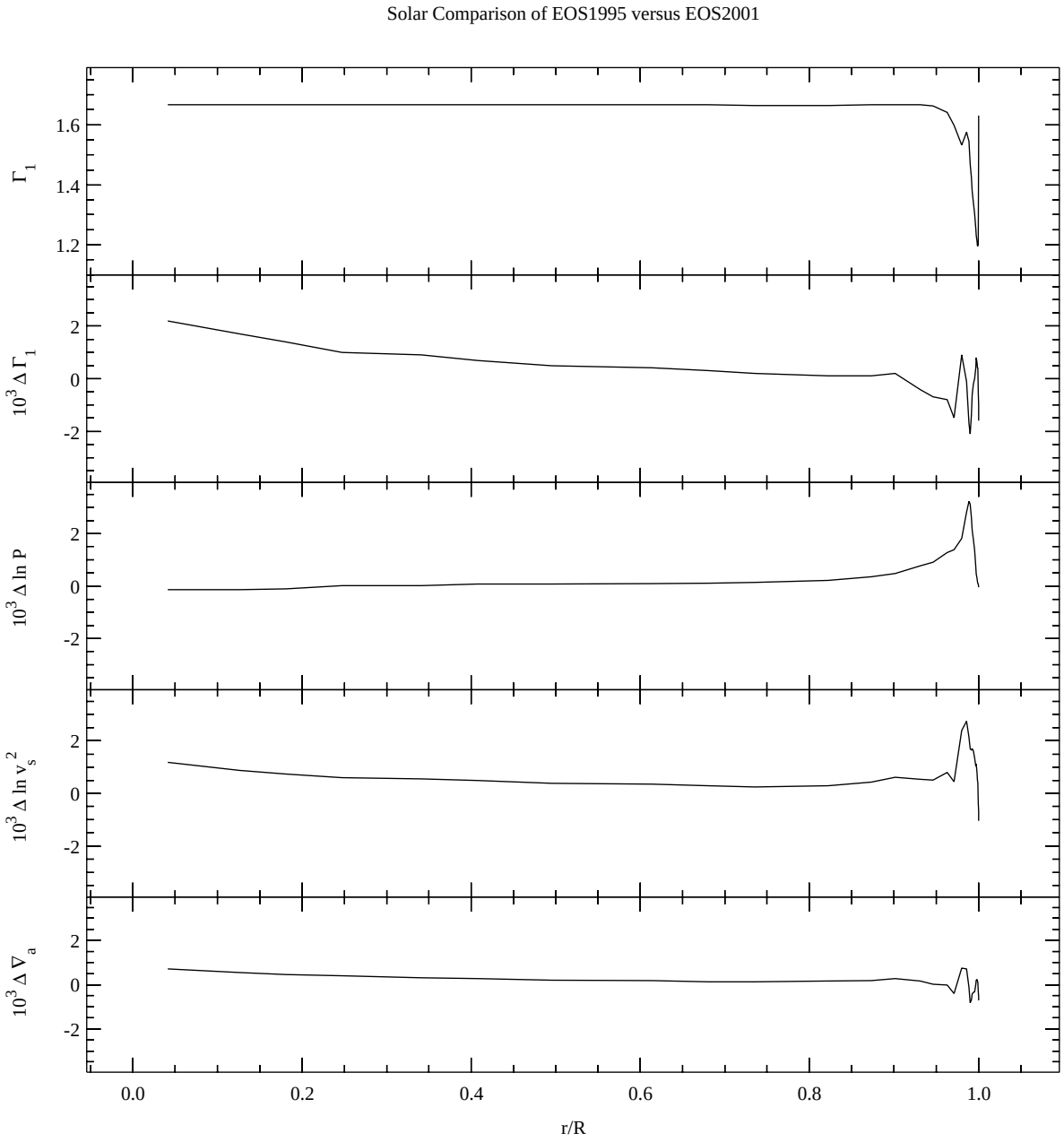
Solar Comparison of EOS1995 versus EOS2001
Γ1
1.6
1.4
1.2
10^3 Δ Γ1
2
0
-2
10^3 Δ ln P
2
0
-2
10^3 Δ ln v_s^2
2
0
-2
10^3 Δ ∇a
2
0
-2
0.0
0.2
0.4
0.6
0.8
1.0
r/R

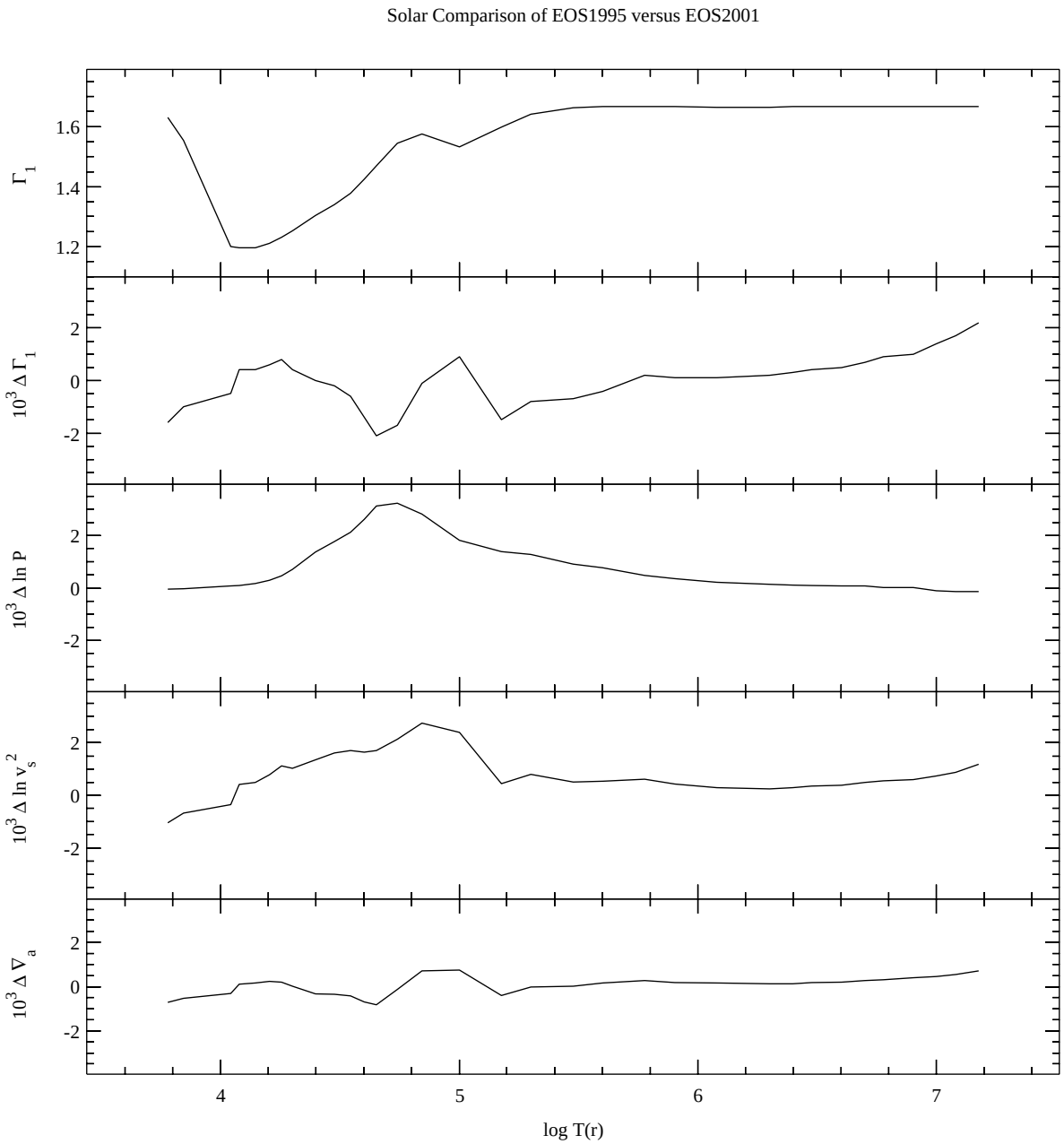
Solar Comparison of EOS1995 versus EOS2001
Γ1
1.6
1.4
1.2
10^3 Δ Γ1
2
0
-2
10^3 Δ ln P
2
0
-2
10^3 Δ ln v_s^2
2
0
-2
10^3 Δ ∇a
2
0
-2
4
5
6
7
log T(r)

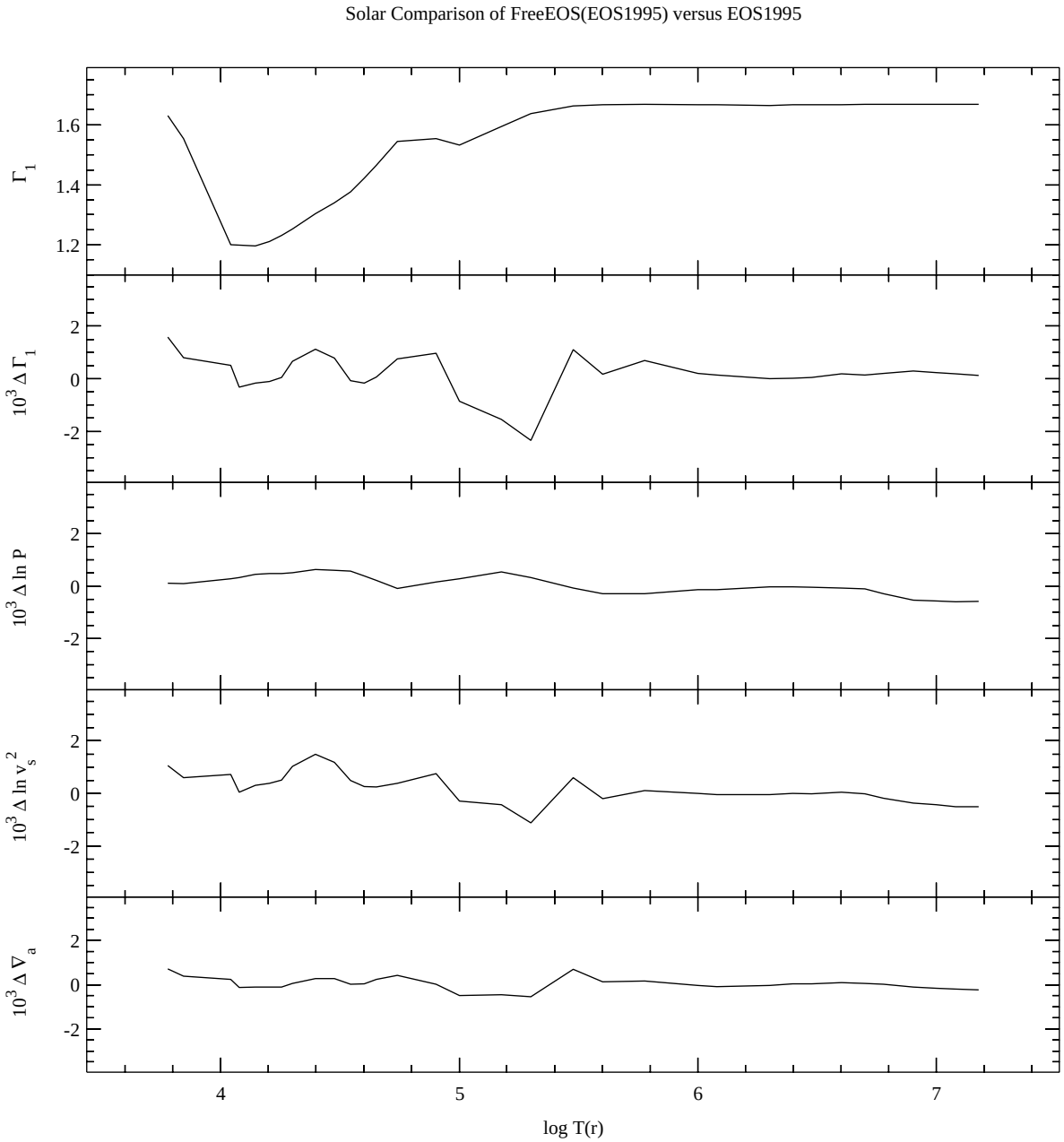
Solar Comparison of FreeEOS(EOS1995) versus EOS1995
Γ1
1.6
1.4
1.2
10^3 Δ Γ1
2
0
-2
10^3 Δ ln P
2
0
-2
10^3 Δ ln v_s^2
2
0
-2
10^3 Δ ∇a
2
0
-2
4
5
6
7
log T(r)

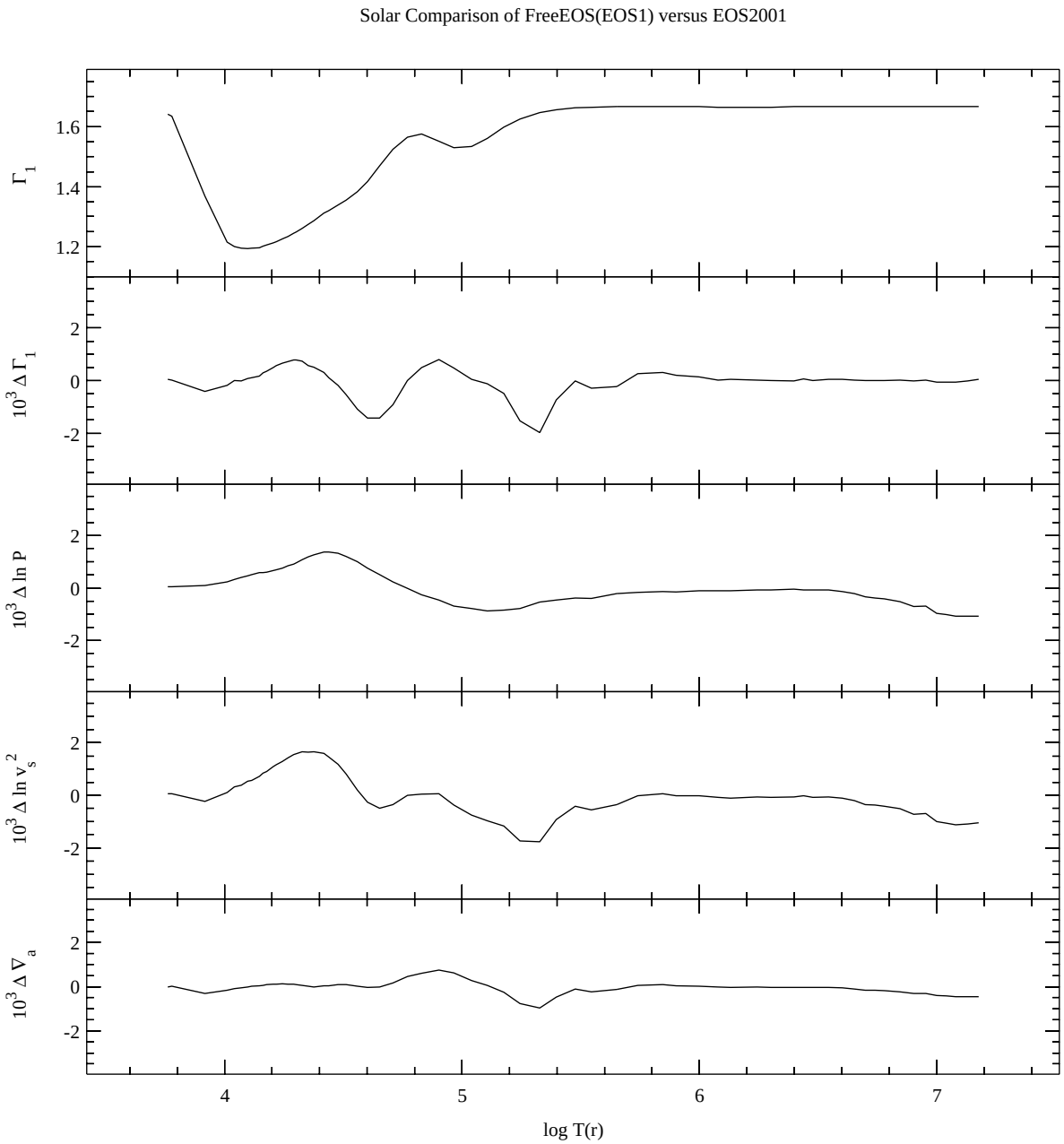
Solar Comparison of FreeEOS(EOS1) versus EOS2001
Γ1
10^3 Δ Γ1
10^3 Δ ln P
10^3 Δ ln v_s^2
10^3 Δ ∇a
log T(r)